Prediction of Active Drug Plasma Concentrations Achieved in Cancer Patients by Pharmacodynamic Biomarkers Identified from the Geo Human Colon Carcinoma Xenograft Model

Feng R. Luo,[1] Zheng Yang,[2] Huijin Dong,[3] Amy Camuso,[1] Kelly McGlinchey,[1] Krista Fager,[1] Christine Flefleh,[1] David Kan,[1] Ivan Inigo,[1] Stephen Castaneda,[1] Tai W. Wong,[1] Robert A. Kramer,[1] Robert Wild,[1] and Francis Y. Lee[1]

Abstract

Purpose: Epidermal growth factor receptor (EGFR), a protein tyrosine kinase expressed in many types of human cancers, has been strongly associated with tumor progression. Cetuximab is an IgG_1 anti-EGFR chimeric mouse/human monoclonal antibody that has been approved for the treatment of advanced colon cancer. Using human tumor xenografts grown in nude mice, we have determined the *in vivo* pharmacodynamic response of cetuximab at efficacious doses. Three pharmacodynamic end points were evaluated: tumoral phospho-EGFR, tumoral mitogen-activated protein kinase (MAPK) phosphorylation, and Ki67 expression.

Experimental Design: The pharmacodynamic study was conducted in nude mice bearing Geo tumors following a single i.p. administration of 0.25 and 0.04 mg. The tumors were analyzed by immunohistochemistry. The levels of phospho-EGFR were quantitated by an ELISA assay.

Results: At 0.25 mg, phospho-EGFR was maximally inhibited by 91% at 24 hours, whereas the level of inhibition decreased to 72% by 72 hours. At 0.04 mg, the maximum inhibition of phospho-EGFR was 53% at 24 hours, whereas the level of inhibition decreased to 37% by 72 hours. The time course of phospho-EGFR inhibition and recovery seemed to correlate with the pharmacokinetics of cetuximab. Immunohistochemical analysis showed that phospho-MAPK and Ki67 expression were inhibited between 24 and 72 hours at 0.25 and 0.04 mg. A pharmacokinetic/pharmacodynamic model was established and predicted that the plasma concentration of cetuximab required to inhibit 90% of phospho-EGFR was 67.5 μg/mL.

Conclusions: Phospho-EGFR/phospho-MAPK could be useful clinical biomarkers to assess EGFR inhibition by cetuximab.

Epidermal growth factor receptor (EGFR) kinase is a 170 kDa plasma membrane glycoprotein composed of an extracellular ligand–binding domain, a transmembrane lipophilic segment, and an intracellular protein kinase domain with a regulatory carboxyl terminal segment (1). Binding of ligand to EGFR results in receptor dimerization, autophosphorylation of specific tyrosine residues within the COOH terminus of EGFR, and the activation of EGFR kinase activity (1, 2). The activation of EGFR kinase initiates a cascade of intracellular signal transduction events involving the activation of mitogen-activated protein kinase (MAPK), which further activates several nuclear proteins required for cell cycle progression from G_1 to S phase (3). EGFR signaling is not only critical for cell proliferation, it also contributes to other crucial processes of cancer progression including angiogenesis, tumor metastasis, and the inhibition of apoptosis (3–5).

Because EGFR pathways are commonly deregulated in human epithelial tumors, therapeutic agents directed at the EGFR represent a promising and important group of molecularly targeted therapies (6, 7). Because tyrosine kinases are also important in many signaling pathways involved in normal cellular functions, the inhibition of EGFR with potent and highly selective monoclonal antibody becomes an attractive therapeutic approach. The first generation of mouse monoclonal antibodies was discovered in the 1980s, it showed the inhibition of ligand-activated EGFR kinase activity and the inhibition of tumor proliferation (8–11). To avoid the potential immune-response in humans, a chimeric human-mouse monoclonal antibody 225 (IMC-225, cetuximab) cont aining a human IgG_1 was subsequently developed for clinical application (12, 13). Cetuximab binds to EGFR with a greater affinity than EGFR natural ligands and is able to block the ligand-induced activation of EGFR (12, 14). It also inhibits the growth of cancer cells expressing EGFR

Authors' Affiliations: [1]Oncology Drug Discovery, [2]Preclinical Candidate Optimization, and [3]Clinical Discovery, Pharmaceutical Research Institute, Bristol-Myers Squibb, Princeton, New Jersey

Received 2/17/05; revised 4/1/05; accepted 5/5/05.

The costs of publication of this article were defrayed in part by the payment of page charges. This article must therefore be hereby marked *advertisement* in accordance with 18 U.S.C. Section 1734 solely to indicate this fact.

Note: F. Luo and Z. Yang contributed equally to this work.

Requests for reprints: Feng Luo, Oncology Drug Discovery, Pharmaceutical Research Institute, Bristol-Myers Squibb Company, Mailstop K23-03, P.O. Box 4000, Princeton, NJ 08543. Phone: 609-252-3558; Fax: 609-252-6051; E-mail: roger.luo@bms.com.

in culture (15–17) as well as in human carcinoma xenografts accompanied by a significant increase in survival of mice (12, 14, 16, 18). Most importantly, clinical studies have shown that cetuximab is able to significantly inhibit tumor growth in cancer patients (19). In 2004, cetuximab was approved by the Food and Drug Administration for the treatment of advanced colon cancer in combination with CPT-11.

When cetuximab was initially tested in cancer patients, three consecutive phase I clinical trials were carried out, in which cetuximab was administered as (*a*) a single i.v. infusion; (*b*) weekly multiple infusion for 4 weeks; (*c*) and weekly multiple infusion in combination with cisplatin (20). The maximum tolerated dose was not reached in any of these studies. Noncompartmental analysis of pharmacokinetic data for dose levels of 20, 50, and 100 mg/m^2 showed that the systemic clearance decreased with increasing dose, whereas the volume of distribution (V_d) at steady state remained relatively constant and approximated to the plasma volume. At dose levels of 200 and 400 mg/m^2, cetuximab achieved a complete saturation of clearance. On the basis of observed complete saturation of clearance, the recommended dosing regimen for further phase II/III trial is a 400 mg/m^2 loading dose, followed by a 250 mg/m^2 weekly maintenance dose. However, there has not been any rigorous experimental evidence to show optimal target inhibition under the recommended dosing regimen.

To develop molecularly targeted agents such as cetuximab and gefitinib, it is extremely valuable to establish a well-understood pharmacologic biomarker, through preclinical studies, that link all of the following essential variables of drug action, from the molecular target to clinical effect: (*a*) the expression or status of the molecular target; (*b*) achievement of the active plasma concentration of drug; (*c*) demonstration of activity against the intended molecular target; (*d*) the modulation of the biochemical pathway in which the molecular target functions; (*e*) the induction of the downstream biological effect (e.g., antiproliferation); and (*f*) the achievement of a clinical response. In general, EGFR/cetuximab, on the basis of their well-understood tumor biology and pharmacology, stand out to be ideal candidates to conduct pharmacokinetic/pharmacodynamic studies in animal models to correlate the aforementioned variables. In particular, the tyrosine residue 1068 within the COOH terminus of EGFR becomes autophosphorylated upon activation of EGFR kinase by its natural ligand, whereas the phosphorylated tyrosine 1068, pY1068, plays an essential role in subsequent receptor internalization of EGFR and activation of the MAPK signaling pathway (21, 22). Furthermore, we have conducted an *in vivo* efficacy study to define the efficacious dose range of cetuximab in Geo human colon tumor xenografts grown in nude mice (23). Therefore, the current study was designed to evaluate (*a*) the phosphorylation status of tyrosine 1068, phospho-EGFR[pY1068], in Geo tumor xenografts *in vivo*; (*b*) whether the inhibition of the tumoral phospho-EGFR[pY1068] correlates with the inhibition of EGFR signaling as well as with the antiproliferative effects by cetuximab at efficacious doses; (*c*) whether the levels of phospho-EGFR/phospho-MAPK could serve as surrogate biomarkers to assess EGFR inhibition by cetuximab.

Materials and Methods

Chemical reagents and antibodies. Complete protease inhibitor tablets were from Roche Diagnostics (Indianapolis, IN). Rabbit anti-mouse IgG and MicroBCA reagents were from Pierce (Rockford, IL). Anti-phosphotyrosine antibody (PY20) and anti-MAPK antibody (sc-94) were purchased from Santa Cruz Biotechnology (Santa Cruz, CA). Mouse monoclonal anti-phospho-EGFR[pY1068] antibody (catalogue 2236) and rabbit polyclonal anti-phospho-MAPK (catalogue 9101) were purchased from Cell Signaling (Beverly, MA). Mouse monoclonal anti-EGFR antibody was purchased from Zymed Laboratories, Inc. (South San Francisco, CA). Anti-rabbit IgG antibody conjugated with horseradish peroxidase was purchased from BD Bioscience (Lexington, KY). Unless otherwise specified, all other chemicals and reagents were from Sigma (St. Louis, MO). Sterile buffers and solutions were obtained from Life Technologies (Carlsbad, CA). Sterile tissue culture ware was obtained from Fisher Scientific Co. (Hanover Park, IL).

Animals. Female, nude mice, 5 to 6 weeks of age, were obtained from Harlan Sprague-Dawley Co. (Indianapolis, IN), and maintained in an ammonia-free environment in a defined and pathogen-free colony. Animals were quarantined for ~3 weeks prior to their use for tumor propagation and drug efficacy testing. They were given food and water ad libitum. Tumors were propagated in nude mice as s.c. transplants using tumor fragments obtained from donor mice. Tumor passage occurred approximately every 2 to 4 weeks. Tumors were then allowed to grow to the predetermined size range (usually between 100 and 200 mg, tumors outside the range were excluded) and animals were evenly distributed to various treatment and control groups. All studies were done in accordance with Bristol-Myers Squibb and the American Association for Accreditation of Laboratory Animal Care protocols.

Drug formulation and administration. Cetuximab (lot 00C01178) was supplied by Imclone Systems, Inc. (New York, NY) at a concentration of 2 mg/mL in a buffer consisting of 10 mmol/L sodium phosphate and 145 mmol/L sodium chloride (pH 7). For the pharmacodynamic study requiring lower concentrations of cetuximab, the stock solution was diluted with sterile PBS (pH 7.4). Cetuximab was administered i.p. at a constant volume of 0.5 mL.

Western analysis of the phospho-EGFR[pY1068] and total EGFR in tumor xenograft samples. Mice bearing Geo xenografts (n = 3) were given a single i.p. dose of cetuximab. Tumors were surgically removed and split in half at the indicated time points. One-half of the tumor was immediately snap-frozen in liquid nitrogen and stored at −80°C until analysis. Frozen tumors were then lysed in ice-cold TTG lysis buffer [1% Triton X-100, 5% glycerol, 20 mmol/L Tris (pH 7.7), 1 mmol/L EDTA, 0.15 mol/L NaCl, 1 mmol/L sodium orthovanadate, 40 μmol/L ammonium molybdate, and 2% complete protease inhibitor]. The total protein concentration of tumor lysate was determined using the MicroBCA method (Pierce). Prior to SDS-PAGE, 10 μL of lysate with 10 μg of total proteins were denatured by boiling with 10 μL of Laemmli SDS sample buffer (Bio-Rad Laboratories, Hercules, CA), further resolved on 7.5% SDS-PAGE gels and transferred to Immobilon-P polyvinyl membrane (Millipore Corp, Bedford, MA) at a constant voltage at 4°C overnight. To detect phospho-EGFR, the membrane was blocked with 5% blotto (Bio-Rad Laboratories) for 30 minutes at 37°C in TBST buffer [10 mmol/L Tris (pH 7.7), 120 mmol/L NaCl, 1 mmol/L EDTA, 0.2% Tween 20], and was subsequently probed with a rabbit polyclonal anti-phospho-EGFR[pY1068] (1:1,000 dilution) for 30 minutes at 37°C, then with an anti-rabbit IgG antibody conjugated with horseradish peroxidase. The phosphoprotein was visualized by chemiluminescence reagent ECL Plus (Amersham Pharmacia Biotech, Piscataway, NJ). The molecular size of EGFR was estimated by comparison with prestained protein precision markers. To detect the total EGFR expression, the same blot was stripped with a stripping buffer [7 mol/L guanidine-HCl, 50 mmol/L glycine (pH 10.3), 0.05 mmol/L EDTA, 0.1 mol/L KCl, 20 mmol/L 2-mercaptoethanol] at room temperature for 10 minutes and probed with rabbit polyclonal

anti-EGFR antibody (1:1,000 dilution) under the same conditions described above.

Quantitation of the total EGFR and phospho-EGFR[pY1068] levels in tumor xenograft samples. Tumor lysates were adjusted to a concentration of 3 mg/mL protein. An equal amount of total protein (30 μg) from each tumor sample was used to analyze the levels of the total EGFR and phospho-EGFR by the ELISA assay according to the protocol recommended by the manufacturer (Biosource International Inc., Camarillo, CA). The level of phospho-EGFR was normalized by the level of total EGFR in each tumor sample. The percentage of inhibition of phospho-EGFR was calculated using the normalized values of the phospho-EGFR.

Immunohistochemical analysis. Upon surgical removal and splitting, the tumor was immediately fixed in 10% neutral formalin and embedded in paraffin. Five micrometer sections were prepared and mounted on positively charged glass slides (VWR, Plainfield, NJ). After deparaffinization in xylene and graded alcohol, the tissue sections were rehydrated and processed for antigen retrieval. For staining with the anti-phospho-MAPK antibody, the sections were submerged in 1× High pH Target Retrieval Solution (DakoCytomation, Carpinteria, CA) and were treated in a pressure cooker for 15 minutes. Sections to be stained with antibodies to MAPK and Ki67 were treated similarly, except that antigen retrieval was done in 1 mmol/L EDTA for MAPK or 10 mmol/L citrate buffer (pH 6) for Ki67. Endogenous peroxidase activity was quenched by 3% hydrogen peroxide in PBS for 10 minutes. The slides were then incubated overnight at 4°C with the following primary antibodies: anti-MAPK at 1:1,500 dilution, anti-phospho-MAPK at 1:250 dilution, or anti-Ki67 at 1:50 dilution. This was followed by incubation with biotinylated goat anti-mouse or anti-rabbit secondary antibodies (Vector Labs, Burlingame, CA) at 1:200 dilution for 30 minutes at room temperature. The slides were further incubated with Vectastain ABC Elite Kit and then with the peroxidase substrate 3,3′-diaminobenzidine (Vector Labs).

Pharmacokinetic and pharmacodynamic modeling. The pharmacokinetic and pharmacodynamic data were analyzed sequentially using the SAAM II software (Seattle, WA). The plasma concentrations of cetuximab following i.v. and i.p. administration were simultaneously fitted using a one-compartment model with first-order absorption kinetics, which can be described by the following integrated equation:

$$C_{\text{i.v.}} = \frac{D_{\text{i.v.}}}{V_{\text{d}}}\left(e^{-k_{\text{el}}\cdot t}\right) \qquad (A)$$

$$C_{\text{i.p.}} = \frac{k_{\text{a}}\cdot D_{\text{i.p.}}\cdot F_{\text{i.p.}}}{V_{\text{d}}\cdot(k_{\text{a}}-k_{\text{el}})}\left(e^{-k_{\text{el}}\cdot t}-e^{-k_{\text{a}}\cdot t}\right) \qquad (B)$$

where k_{el} is the elimination rate constant, V_{d} is the volume of distribution, D stands for dose, k_{a} is the absorption rate constant, and F stands for bioavailability. The estimated pharmacokinetic variables were then linked with the pharmacodynamic model as well as to simulate the pharmacokinetic profile for the multiple dosing schedule.

The percentage of inhibition of phospho-EGFR was used as the pharmacodynamic response of cetuximab in pharmacodynamic modeling with an indirect inhibitory $E_{\max}$ model. In the absence of cetuximab, the rate of changes in the phospho-EGFR level can be described by the following equation:

$$\frac{dR_0}{dt} = k_{\text{in}} - k_{\text{out}}\cdot R_0 \qquad (C)$$

where R_0 is the baseline value of phospho-EGFR, k_{in} is the zero-order rate constant for the formation of phospho-EGFR, k_{out} is the first-order rate constant of dephosphorylation of phospho-EGFR. In the absence of cetuximab, the phospho-EGFR level was assumed to be at steady sate, at which the rate of phospho-EGFR formation (k_{in}) was equal to the rate of dephosphorylation of phospho-EGFR ($k_{\text{out}} \times R_0$).

$$k_{\text{in}} = k_{\text{out}}\cdot R_0 \qquad (D)$$

In the presence of cetuximab, it was assumed that the reduction of phospho-EGFR was primarily due to the inhibition by drug instead by endogenous phosphatases. The percentage of phospho-EGFR relative to the baseline value (i.e., R/R_0) in the presence of cetuximab was described by the following equation:

$$\frac{d(R/R_0)}{dt} = \frac{k_{\text{in}}}{R_0}\cdot\left(1-\frac{E_{\max}\cdot C_{\text{i.p.}}}{\text{EC}_{50}+C_{\text{i.p.}}}\right) - k_{\text{out}}\cdot(R/R_0) \qquad (E)$$

where $E_{\max}$ was the maximum inhibitory response and was assumed to be 100% in the model, and EC_{50} is the drug concentration corresponding to 50% of $E_{\max}$. Substituting Eq. D into Eq. E, it yielded:

$$\frac{d(R/R_0)}{dt} = k_{\text{out}}\cdot\left(1-\frac{C_{\text{i.p.}}}{\text{EC}_{50}+C_{\text{i.p.}}}\right) - k_{\text{out}}\cdot(R/R_0) \qquad (F)$$

Eq. F was then used to simultaneously fit the pharmacodynamic data. Goodness of fit was assessed by the minimization of the objective function, Akaike and Schwarz-Bayesian information criteria, visual inspection of the fitting and residual plots, and the precision of the variables estimated.

Results

Pharmacodynamics of cetuximab in nude mice bearing Geo tumor xenografts. We have conducted efficacy studies to define the optimal biological dose and the minimum effective dose of cetuximab in nude mice bearing Geo human colon xenografts (23). It was observed that cetuximab was equally active at dose levels ranging from 1 to 0.25 mg, whereas inhibiting the tumor growth dose-dependently at levels of 0.25, 0.1, and 0.04 mg. Therefore, cetuximab dose levels of 0.25 mg or higher were suggested to be optimal for the antitumor activity. The dose of 0.04 mg was active but much less efficacious than 0.25 mg, and therefore was considered suboptimal or close to the minimum effective dose. Our observation was consistent with the observations by other investigators using the same tumor model (16, 24). In the present study, pharmacodynamic biomarkers of cetuximab were determined using the same tumor model at dose levels of 0.25 and 0.04 mg.

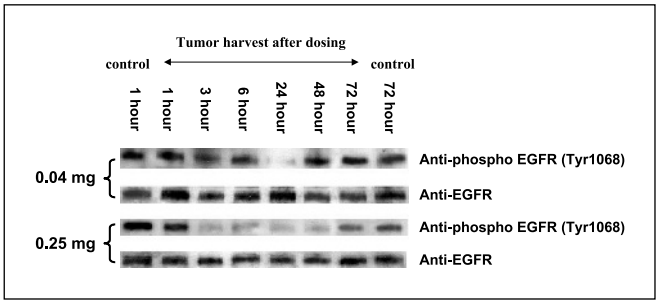

Fig. 1. Inhibition of the phosphorylation of EGFR in the Geo tumor xenograft following a single i.p. injection of cetuximab at 0.04 and 0.25 mg. Tumors were surgically removed, immediately snap-frozen in liquid nitrogen and stored at −80°C until Western analysis.

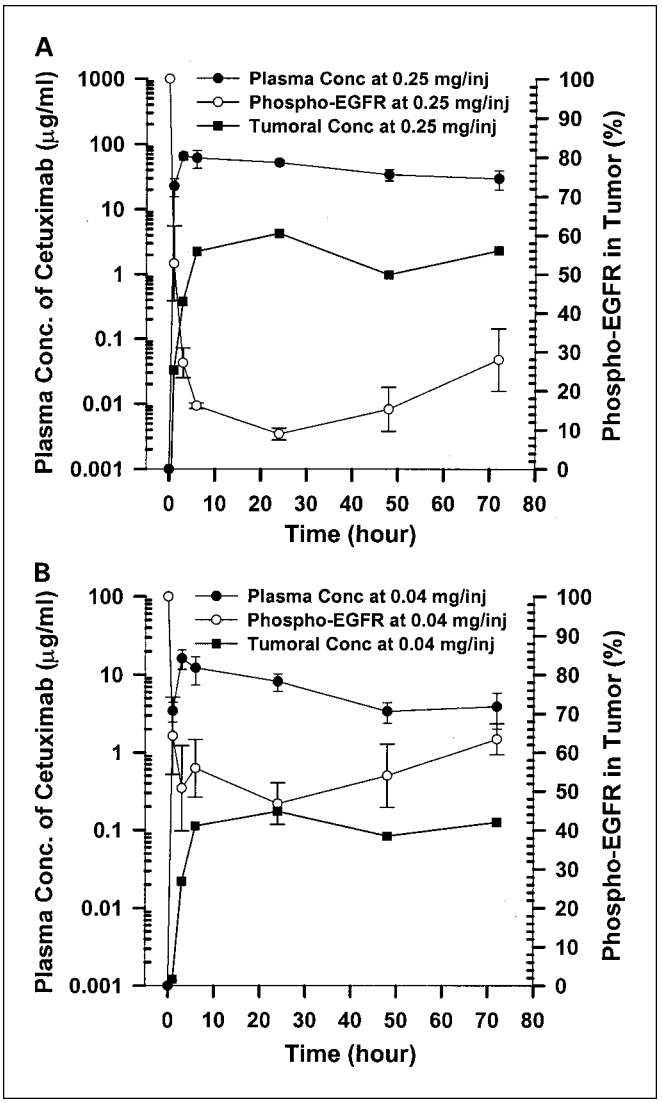

Fig. 2. *A* and *B*, pharmacodynamics of cetuximab in the Geo tumor-bearing mice following a single i.p. administration at 0.25 and 0.04 mg. Nude mice bearing human Geo tumor following a single i.p. administration at dose levels of 0.25 and 0.04 mg. Tumors were surgically removed at 0, 1, 3, 6, 24, 48, and 72 hours and immediately frozen in liquid nitrogen and stored at −80°C until Western analysis. The inhibition of the activated EGFR was quantitated by an ELISA assay. *Points*, means; *bars*, ±SD. Pharmacokinetic data were quoted from our previous publication (23).

Tumoral phospho-EGFR was analyzed by Western blot analysis with a phospho-specific antibody anti-EGFR[pY1068]. It was shown that tumoral phospho-EGFR was inhibited at both doses, but the extent and duration of tumoral phospho-EGFR inhibition appeared different (Fig. 1). The inhibition of tumoral phospho-EGFR was quantitated by the ELISA assay and plotted versus time (Fig. 2). At 0.25 mg, tumoral phospho-EGFR was maximally inhibited by 91% at 24 hours post-dose, whereas the level of inhibition declined progressively to 72% by 72 hours post-dose. Because the *in vivo* efficacy study of cetuximab was conducted with a multiple dosing schedule (q3dx5; ref. 23), the inhibition of tumoral phospho-EGFR would be conceivably ≥72% throughout the treatment period at dose levels of ≥0.25 mg. At 0.04 mg, the maximum inhibition of tumoral phospho-EGFR was 53% at 24 hours, whereas the level of the inhibition was reversed to 37% by 72 hours. In general, the time course of tumoral phospho-EGFR inhibition and recovery seemed to correlate with plasma and tumoral levels of cetuximab at 0.25 and 0.04 mg (Fig. 2). The expression level of the total EGFR was not significantly modified at either dose, indicating that the inhibition of tumoral phospho-EGFR was primarily due to the reduction of ligand-induced EGFR activation in tumor.

MAPK is one of the most well-characterized downstream components of the EGFR signaling pathway, and therefore, could serve as an important surrogate biomarker of the activated EGFR kinase (25). Hence, we measured the phosphorylation status of MAPK in tumor by immunohistochemistry (Fig. 3A). It was observed that tumoral phospho-MAPK was inhibited at both 0.25 and 0.04 mg, paralleling the inhibition of tumoral phospho-EGFR by cetuximab. The time course of tumoral phospho-MAPK seemed, in general, consistent with the pharmacokinetics of cetuximab at 0.25 and 0.04 mg. The inhibition of tumoral phospho-MAPK was believed to be mediated by the inhibition of the EGFR pathway because cetuximab is a potent and specific inhibitor of EGFR kinase (12, 14). To determine the tumor growth inhibitory effect of cetuximab, tumor cell proliferation was assessed with a commonly used marker Ki-67, a proliferation-associated antigen present only in proliferating cells (26, 27). The inhibition of Ki67 expression was also observed at both 0.25 and 0.04 mg (Fig. 3B). It seemed that Ki67 expression was similarly inhibited at 24 and 48 hours for both doses, whereas, at 72 hours, the inhibition of Ki67 expression became less for 0.04 mg than for 0.25 mg, suggesting a greater tumor growth inhibition was likely achieved at 0.25 than at 0.04 mg. Essentially, the tumor growth-inhibitory effect of cetuximab, assessed by Ki67 expression, is consistent with the antitumor activity of cetuximab determined *in vivo* (23). Collectively, our study suggested that cetuximab is able to modulate EGFR kinase activity in tumor and to inhibit tumor proliferation consequently; whereas the tumoral levels of phospho-EGFR/phospho-MAPK could serve as pharmacodynamic biomarkers assessing target inhibition by cetuximab.

Estimation of active drug concentration by pharmacokinetic/pharmacodynamic modeling. Because cetuximab does not bind to mouse EGFR (9), its distribution is likely confined in the plasma compartment. Therefore, a one-compartment model with the first-order absorption kinetics was applied in pharmacokinetic modeling. The pharmacokinetic model was simultaneously fitted to the plasma concentrations of mice given a single dose of cetuximab i.v. and i.p. at 1.0, 0.25, and 0.04 mg (Fig. 4). The constants of k_a and k_d were estimated to be 0.44 ± 0.09 and 0.017 ± 0.002 $hour^{-1}$, respectively, whereas the V_d was 0.094 ± 0.003 L/kg. The percentage inhibition of tumoral phospho-EGFR by cetuximab was used as the pharmacodynamic response in pharmacodynamic modeling. It was assumed that the level of tumoral phospho-EGFR was at steady state in the absence of cetuximab, whereas the reduction of tumoral phospho-EGFR when cetuximab was administered was primarily due to the inhibition of phospho-EGFR by drug. When the inhibition of tumoral phospho-EGFR was plotted versus the plasma concentration of cetuximab at both 0.25 and 0.04 mg, hysteresis was observed, suggesting that there was a delay between the plasma concentration and the inhibition of

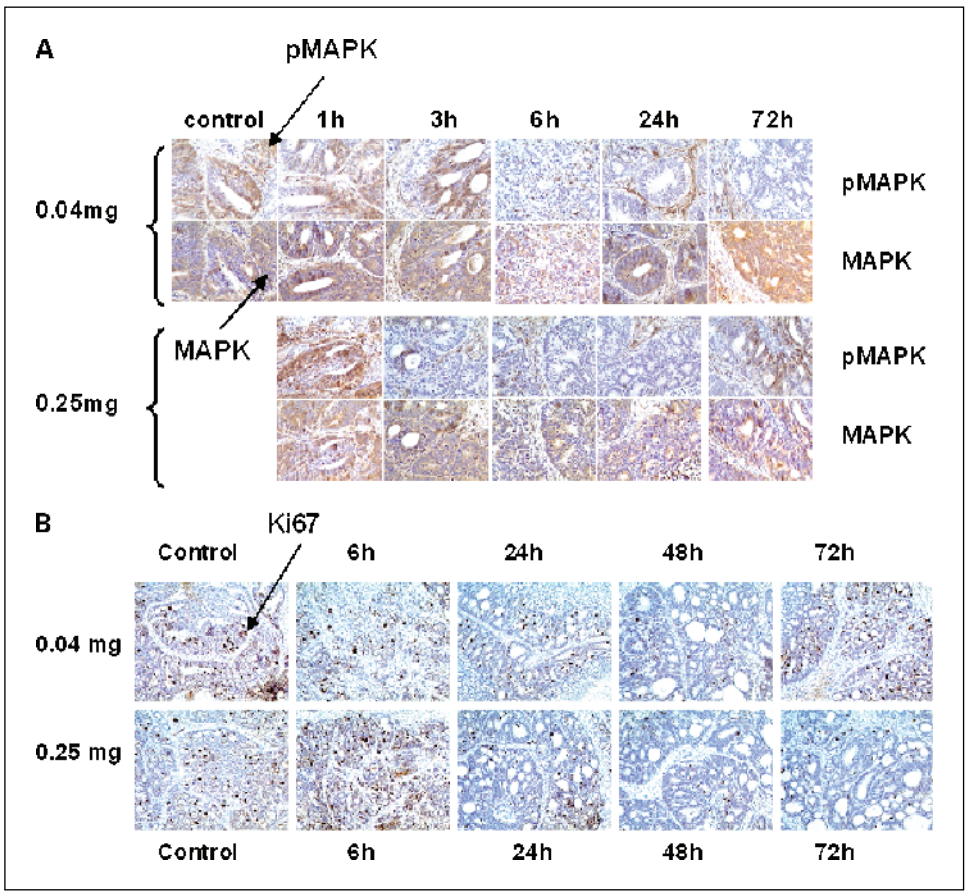

Fig. 3. Inhibition of the phosphorylation of MAPK (*A*) and Ki-67 expression (*B*) in the Geo tumor xenograft following a single i.p. injection of cetuximab at 0.25 or 0.04 mg. Tumors were surgically removed, immediately fixed in 10% neutral formalin, embedded in paraffin and analyzed immunohistochemically.

tumoral phospho-EGFR by cetuximab (data not shown). Therefore, an indirect inhibitory E_{max} model was applied in pharmacodynamic modeling. The pharmacodynamic model linked with the defined pharmacokinetic model was simultaneously fitted to the pharmacodynamic data to estimate the active plasma concentration of cetuximab (Fig. 5). The value of EC_{50}, the plasma concentration required to inhibit 50% of tumoral phospho-EGFR, was 7.5 ± 0.8 μg/mL.

When the EC_{50} was compared with the simulated plasma profiles of cetuximab with the schedule of q3dx5 (Fig. 6), it was found that the trough plasma levels of cetuximab, when given at the suboptimal dose of 0.04 mg, were around the EC_{50}, implying ~50% of phospho-EGFR at this dose level. Because 0.04 mg is close to the minimum effective dose in our studies, it can be conceived that 50% of target inhibition is probably minimally required for cetuximab in order to be active against Geo tumor. On the other hand, the peak plasma levels of cetuximab at 0.04 mg were well below the EC_{90} (67.5 μg/mL), implying significantly >90% of phospho-EGFR inhibition at 0.04 mg. Therefore, the optimal antitumor activity may not be achieved at 0.04 mg, which was the observation in our *in vivo* efficacy study of cetuximab (23). For 0.25 mg, the trough plasma levels of cetuximab were around or above the EC_{90}, implying that nearly complete, if not 100% inhibition of phospho-EGFR was achieved and a consequent optimal activity could be expected at dose levels of ≥0.25 mg, which was also consistent with the outcome of our efficacy study (23).

Discussion

For many molecularly targeted agents, the clinical dose continues to be defined by traditional means. For small molecule inhibitors of EGFR kinase such as gefitinib or erlotinib, investigators were able to define a maximum tolerated dose associated with dose-limiting toxicity. The further studies were conducted at a lower but tolerable dose, which still has evidence of clinical response (28, 29). However, there remain agents which are associated with minimal toxicity in the clinical setting, such as cetuximab. In these cases, the decision regarding optimal dose needs to be based on other criteria, for example, biomarkers, especially the mechanism-based biomarkers. In general, cetuximab seems to be well-tolerated in clinical studies, whereas a clear maximum tolerated dose has never been reached in contrast to other small molecule inhibitors. The current dosing regimen was recommended based on the clinical observation of a complete saturation of systemic clearance at efficacious doses (20, 30). However, there has not been any rigorous experimental evidence to equate the saturation of systemic clearance to complete inhibitory status of EGFR in tumors under the current clinical dosing regimen. Moreover, the functionally activated EGFR, the predominant driving force for cell proliferation in cetuximab-responsive tumors, could be a portion of total EGFR. This would further imply that the dose required to saturate systemic clearance or total EGFR in tissues could be different from the one required to inhibit the activity of the functional EGFR in tumor.

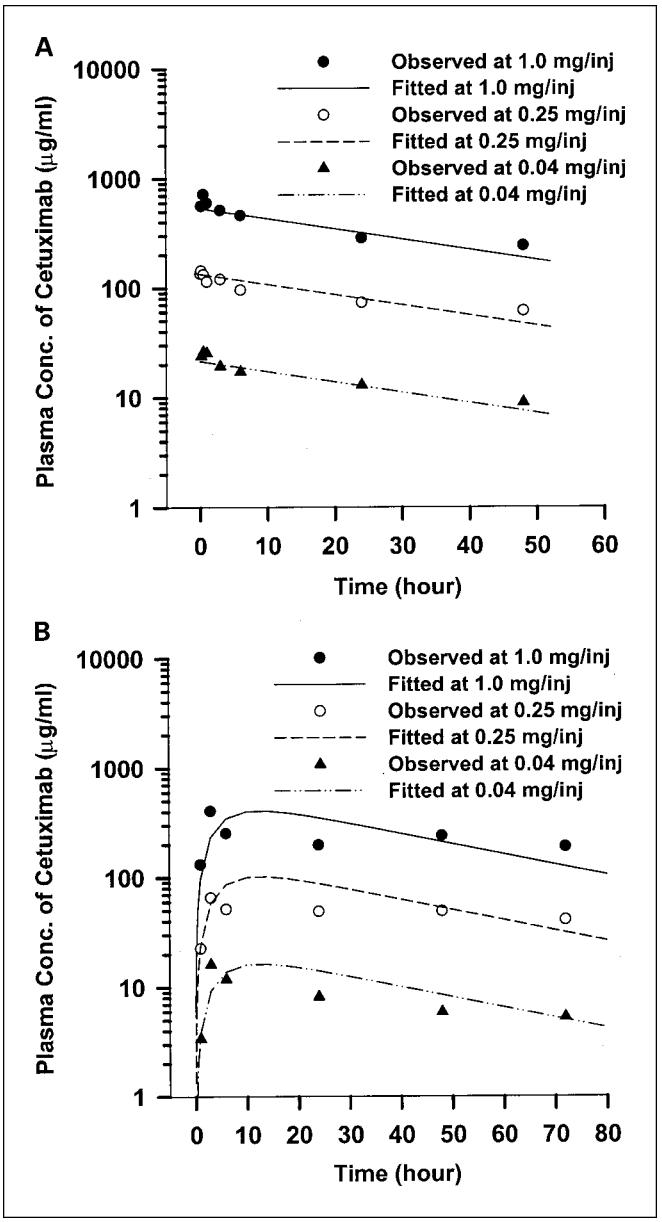

Fig. 4. Pharmacokinetic modeling of cetuximab in mice following a single i.v. (*A*) or i.p. (*B*) injection at 1, 0.25, and 0.04 mg. The pharmacokinetic data were simultaneously fitted using a one-compartment model. The estimated disposition variables were then linked with the pharmacodynamic model.

In the present study, on the basis of the thorough understanding of EGFR signaling and the clinical experience of cetuximab, we proposed phospho-EGFR/phospho-MAPK as the mechanism-based pharmacodynamic biomarker to assess target exposure. At dose levels of 0.25 and 0.04 mg, a dose-dependent inhibition of phospho-EGFR was observed for cetuximab. The time course of phospho-EGFR inhibition and recovery correlated with the plasma levels of cetuximab at both doses. This essentially supported the hypothesis that the level of tumoral phospho-EGFR could be used as an *in vivo* biomarker assessing target exposure of cetuximab. MAPK is one of the most well-characterized cell proliferative components of the EGFR signaling pathway. The inhibition of phospho-EGFR by cetuximab has been clearly linked with the phosphorylation status of MAPK in cells and with subsequent pharmacologic end points such as tumor cell proliferation or apoptosis (31–34). Particularly, in patients with head and neck tumors, a strong correlation has been shown, upon treatment with cetuximab, between the inhibition of phospho-MAPK and the inhibition of EGFR kinase activity in tumor and skin tissues (33). Therefore, we further investigated the level of tumoral phospho-MAPK in the present study. It was found that tumoral phospho-MAPK was inhibited at both 0.25 and 0.04 mg, which correlated with the inhibition of tumoral phospho-EGFR. In general, the time course of phospho-MAPK inhibition and recovery seemed to correlate with the plasma levels of cetuximab, similar to that of phospho-EGFR. Because the inhibition of phospho-MAPK has been reported to correlate with anti-proliferation in tumor assessed by Ki67 expression (33), we further determined the tumoral Ki67 expression. It seemed that the tumoral Ki67 expression was inhibited dose-dependently, which paralleled the inhibition of tumoral phospho-EGFR/phospho-MAPK. Essentially, our study suggested that cetuximab is able to modulate the activity of the EGFR kinase in tumor and consequently to inhibit tumor proliferation. In general, phospho-MAPK has been more extensively studied as a biomarker to assess EGFR kinase signaling and inhibition. Take into consideration that MAPK may be activated by several pathways (35–37), phospho-MAPK itself, as a biomarker, may not be sufficient to predict EGFR targeting. Our study suggests that the tumoral levels of phospho-EGFR/phospho-MAPK should be evaluated together to assess the EGFR inhibition by cetuximab.

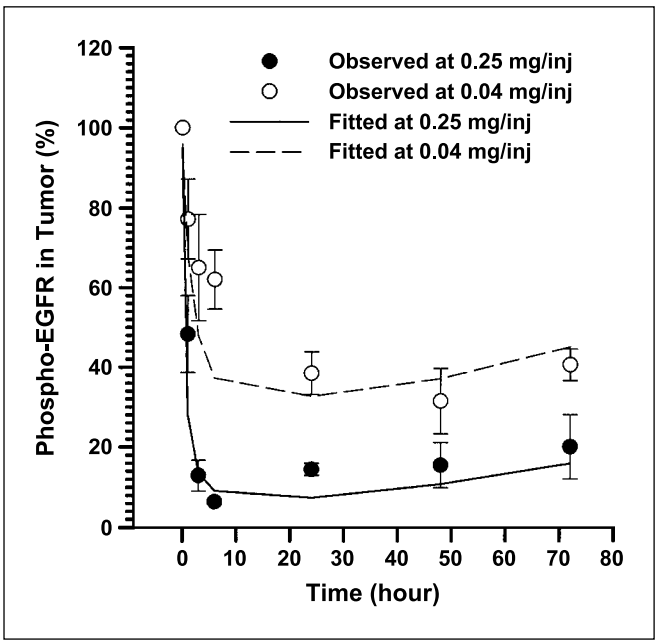

Fig. 5. Pharmacokinetic and pharmacodynamic modeling of cetuximab in Geo tumor-bearing mice following a single i.p. injection at 0.25 and 0.04 mg. The pharmacokinetic data were simultaneously fitted using a one-compartment model with first-order absorption kinetics. The estimated pharmacokinetic variables were then used to link with the pharmacodynamic model. The pharmacodynamic data were simultaneously fitted using an indirect pharmacodynamic model with an assumption that the phosphorylated EGFR level was assumed to be at steady state in the absence of cetuximab. Also, the reduction of the phosphorylated EGFR measured in the experiment was primarily due to the inhibition by drug.

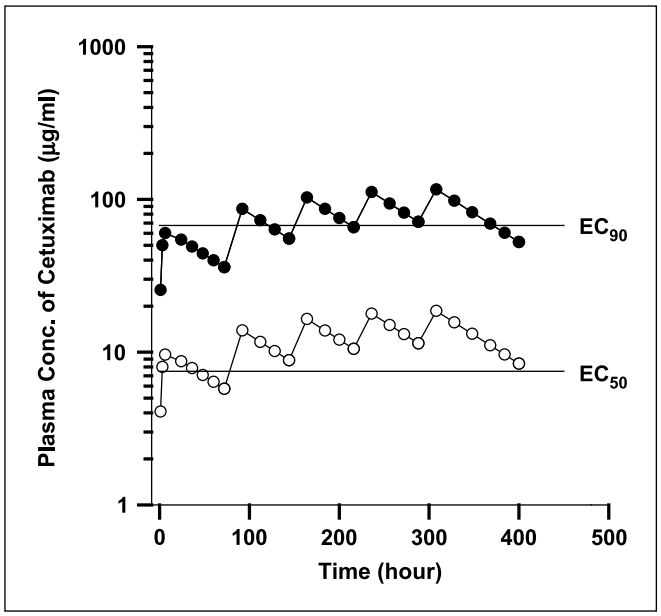

Fig. 6. Simulation of plasma levels of cetuximab in mice with a dosing schedule of q3dx5 at 0.25 and 0.04 mg. The pharmacokinetic data were simultaneously fitted using a one-compartment model with first-order absorption kinetics. The plasma profile was simulated based on an assumption of linear pharmacokinetics for cetuximab with multiple administrations at dose range of 0.25 to 0.04 mg. (●) 0.25 mg, (○) 0.04 mg.

Our pharmacokinetic/pharmacodynamic model predicted the EC_{50}, which is probably required to achieve a minimal antitumor activity of cetuximab, whereas the EC_{90} is more likely to be required for the optimal response. We would recommend that the EC_{90} (67.5 μg/mL) could serve as a conservative measure of the active plasma concentration of cetuximab. A complete inhibition of the active EGFR could be achieved at plasma concentrations of cetuximab >75 μg/mL, i.e., EC_{100}, which can be suggested as active plasma concentrations. When cancer patients were treated with cetuximab at a multiple weekly dose of 400 mg/m^2, the C_{ss} was estimated to be 56 μg/mL (20). When the treatment schedule was a 400 mg/m^2 loading dose followed by a 250 mg/m^2 weekly maintenance dose, the mean peak and trough plasma levels of cetuximab in patients were estimated to be 192 and 75 μg/mL, respectively, whereas the C_{ss} was ~100 μg/mL (38). Therefore, the C_{ss} of cetuximab in cancer patients is likely within the range of 56 to 100 μg/mL under the current clinical dosing regimen. These reported plasma levels of cetuximab have been confirmed in phase II clinical studies being conducted by Bristol-Myers Squibb and its alliances (data not shown). It is interesting that our predicted active plasma concentration of 75 μg/mL is fairly comparable to the C_{ss} achieved in cancer patients. In contrast, when predicting the clinical active dose from the preclinical data, the traditional allometric dose scaling method seemed problematic. The preclinical optimal dose of 0.25 mg, if scaled up based on the formula recommended by Freireich et al. (39) with an assumption of a 70 kg average body weight of patients, is equivalent to a clinical dose of 37.5 mg/m^2, which is significantly below the current clinical dose. This discrepancy could be due to the different routes of drug clearance, i.e., cetuximab only binds to human but not to mouse EGFR, therefore, extra amounts of cetuximab are required for patients to saturate EGFR in a number of tissues, e.g., the skin and liver. Because the inhibition of EGFR directly correlates to the plasma concentration of drug, the different affinities of cetuximab to human and mouse EGFR or the consequent different routes of drug clearance should not affect EGFR inhibition once appropriate concentrations are achieved regardless of species. Therefore, the active plasma concentration, predicted by biomarker, phospho-EGFR inhibition in human tumors grown s.c. in mouse, is more readily translated into clinical studies due to limited impact from affinity difference of the antibody.

It is usually believed that biomarker should be identified and validated in the preclinical stage. The optimal exposure or active drug concentration could therefore be predicted before the drug candidate enters into clinical studies. One may argue the necessity of the present study because cetuximab has been approved by the Food and Drug Administration. However, there have not been enough convincing data to prove that the active drug concentration determined in animal models could provide a useful guide for clinical trials. The present study showed evidence that the active drug concentration, predicted by preclinical pharmacokinetics/biomarkers, correlated with the active concentrations achieved in cancer patients. Our study also suggests that EGFR is likely to be significantly, if not completely, blocked by cetuximab in cancer patients under the current clinical dosing regimen. Hence, the clinical dose of cetuximab, even though defined not based on biomarkers, probably approximates to the optimal biological dose. The current study was conducted by no means to tackle the clinical regimen of cetuximab, but to strongly advocate that more preclinical pharmacokinetics/biomarker studies should be conducted to define the optimal drug exposure to facilitate clinical drug development. The model established in the present study has been applied in phase I studies in chronic myelogenous leukemia patients treated with a novel SRC/BCR-ABL kinase inhibitor, BMS-354825. In this case, the predicted active concentration from preclinical models was in line with those achieved by patients who also had clinical response to the treatment (40).

Having mentioned some success with our pharmacokinetics/biomarker model, we would also suggest that this model should be used with certain caution before it is extensively evaluated. Phospho-EGFR/phospho-MAPK, as pharmacodynamic biomarkers, are probably adequate to predict the target exposure. In the present study, they probably coincidentally correlated with cetuximab efficacy in the Geo model, which is a sensitive model for cetuximab treatment. In resistant tumor models, one could conceive that EGFR might still be inhibited by cetuximab, but the lack of efficacy could be attributable to either the lower degree of modulation of signaling pathway or activation of survival pathways. Therefore, the current model may not be suitable to predict the overall treatment response of cetuximab. To facilitate clinical drug development, pharmacogenomic and proteomic approaches should also be applied to identify gene or protein biomarkers, which could predict the responsiveness of patients to drug treatment. It has been shown that certain proteins are potentially involved in resistance mechanisms of cetuximab therapy, whereas the different expression levels of

proteins may serve as biomarkers predicting resistance (41). Our colleagues have also identified a set of gene and protein biomarkers predicting response to cetuximab by profiling cetuximab-sensitive and -resistant tumors using pharmacogenomics and proteomics approaches (42, 43). To develop novel molecularly targeted agents, the optimal clinical exposure and regimen should be determined by an array of biomarkers, including target exposure biomarkers and patient selection biomarkers, in combination with clinical responses and toxicity profiles.

References

1. Carpenter G. Receptors for epidermal growth factor and other polypeptide mitogens. Annu Rev Biochem 1987;56:881–914.
2. Sorkin A, McClure M, Huang F, Carter R. Interaction of EGF receptor and grb2 in living cells visualized by fluorescence resonance energy transfer (FRET) microscopy. Curr Biol 2000;10:1395–8.
3. Perry JE, Grossmann ME, Tindall DJ. Epidermal growth factor induces cyclin D1 in a human prostate cancer cell line. Prostate 1998;35:117–24.
4. Mendelsohn J, Baselga J. The EGF receptor family as targets for cancer therapy. Oncogene 2000;19:6550–65.
5. Noonberg SB, Benz CC. Tyrosine kinase inhibitors targeted to the epidermal growth factor receptor subfamily: role as anticancer agents. Drugs 2000;59:753–67.
6. Sporn MB, Roberts AB. Autocrine growth factors and cancer. Nature 1985;313:745–7.
7. Di Marco E, Pierce JH, Fleming TP, et al. Autocrine interaction between TGFα and the EGF-receptor: quantitative requirements for induction of the malignant phenotype. Oncogene 1989;4:831–8.
8. Kawamoto T, Sato JD, Le AD, Polikoff J, Sato GH, Mendelsohn J. Growth stimulation of A431 cells by epidermal growth factor: identification of high-affinity receptors for epidermal growth factor by an anti-receptor monoclonal antibody. Proc Natl Acad Sci U S A 1983;80:1337–41.
9. Sato JD, Kawamoto T, Le AD, Mendelsohn J, Polikoff J, Sato GH. Biological effects *in vitro* of monoclonal antibodies to human epidermal growth factor receptors. Mol Biol Med 1983;1:511–29.
10. Gill GN, Kawamoto T, Cochet C, et al. Monoclonal anti-epidermal growth factor receptor antibodies which are inhibitors of epidermal growth factor binding and antagonists of epidermal growth factor binding and antagonists of epidermal growth factor-stimulated tyrosine protein kinase activity. J Biol Chem 1984;259:7755–60.
11. Masui H, Kawamoto T, Sato JD, Wolf B, Sato G, Mendelsohn J. Growth inhibition of human tumor cells in athymic mice by anti-epidermal growth factor receptor monoclonal antibodies. Cancer Res 1984;44:1002–7.
12. Goldstein NI, Prewett M, Zuklys K, Rockwell P, Mendelsohn J. Biological efficacy of a chimeric antibody to the epidermal growth factor receptor in a human tumor xenograft model. Clin Cancer Res 1995;1:1311–8.
13. Mendelsohn J. Epidermal growth factor receptor inhibition by a monoclonal antibody as anticancer therapy. Clin Cancer Res 1997;3:2703–7.
14. Prewett M, Rockwell P, Rockwell RF, et al. The biologic effects of C225, a chimeric monoclonal antibody to the EGFR, on human prostate carcinoma. J Immunother Emphasis Tumor Immunol 1996;19:419–27.
15. Bruns CJ, Harbison MT, Davis DW, et al. Epidermal growth factor receptor blockade with C225 plus gemcitabine results in regression of human pancreatic carcinoma growing orthotopically in nude mice by antiangiogenic mechanisms. Clin Cancer Res 2000;6:1936–48.
16. Ciardiello F, Bianco R, Damiano V, et al. Antitumor activity of sequential treatment with topotecan and anti-epidermal growth factor receptor monoclonal antibody C225. Clin Cancer Res 1999;5:909–16.
17. Inoue K, Slaton JW, Perrotte P, et al. Paclitaxel enhances the effects of the anti-epidermal growth factor receptor monoclonal antibody ImClone C225 in mice with metastatic human bladder transitional cell carcinoma. Clin Cancer Res 2000;6:4874–84.
18. Prewett M, Rothman M, Waksal H, Feldman M, Bander NH, Hicklin DJ. Mouse-human chimeric anti-epidermal growth factor receptor antibody C225 inhibits the growth of human renal cell carcinoma xenografts in nude mice. Clin Cancer Res 1998;4:2957–66.
19. Mendelsohn J. Antibody-mediated EGF receptor blockade as an anticancer therapy: from the laboratory to the clinic. Cancer Immunol Immunother 2003;52:342–6.
20. Baselga J, Pfister D, Cooper MR, et al. Phase I studies of anti-epidermal growth factor receptor chimeric antibody C225 alone and in combination with cisplatin. J Clin Oncol 2000;18:904–14.
21. Jiang X, Huang F, Marusyk A, Sorkin A. Grb2 regulates internalization of EGF receptors through clathrin-coated pits. Mol Biol Cell 2003;14:858–70.
22. Rodrigues GA, Falasca M, Zhang Z, Ong SH, Schlessinger J. A novel positive feedback loop mediated by the docking protein Gab1 and phosphatidylinositol 3-kinase in epidermal growth factor receptor signaling. Mol Cell Biol 2000;20:1448–59.
23. Luo FR, Yang Z, Dong H, et al. Correlation of pharmacokinetics with the antitumor activity of Cetuximab in nude mice bearing the GEO human colon carcinoma xenograft. Cancer Chemother Pharmacol. In press 2004.
24. Bianco C, Bianco R, Tortora G, et al. Antitumor activity of combined treatment of human cancer cells with ionizing radiation and anti-epidermal growth factor receptor monoclonal antibody C225 plus type I protein kinase A antisense oligonucleotide. Clin Cancer Res 2000;6:4343–50.
25. Barnes CJ, Bagheri-Yarmand R, Mandal M, et al. Suppression of epidermal growth factor receptor, mitogen-activated protein kinase, and Pak1 pathways and invasiveness of human cutaneous squamous cancer cells by the tyrosine kinase inhibitor ZD1839 (Iressa). Mol Cancer Ther 2003;2:345–51.
26. Albanell J, Rojo F, Averbuch S, et al. Pharmacodynamic studies of the epidermal growth factor receptor inhibitor ZD1839 in skin from cancer patients: histopathologic and molecular consequences of receptor inhibition. J Clin Oncol 2002;20:110–24.
27. Cattoretti G, Becker MH, Key G. Monoclonal antibodies against recombinant parts of the Ki-67 antigen (MIB 1 and MIB 3) detect proliferating cells in microwave-processed formalin-fixed paraffin sections. J Pathol 1992;168:357–63.
28. Hidalgo M, Siu LL, Nemunaitis J, et al. Phase I and pharmacologic study of OSI-774, an epidermal growth factor receptor tyrosine kinase inhibitor, in patients with advanced solid malignancies. J Clin Oncol 2001;19:3267–79.
29. Arteaga CL, Johnson DH. Tyrosine kinase inhibitors-ZD1839 (Iressa). Curr Opin Oncol 2001;13:491–8.
30. Baselga J, Mendelsohn J. Receptor blockade with monoclonal antibodies as anti-cancer therapy. Pharmacol Ther 1994;64:127–54.
31. Lenferink AE, Simpson JF, Shawver LK, Coffey RJ, Forbes JT, Arteaga CL. Blockade of the epidermal growth factor receptor tyrosine kinase suppresses tumorigenesis in MMTV/Neu + MMTV/TGF-α bigenic mice. Proc Natl Acad Sci U S A 2000;97:9609–14.
32. Albanell J, Rojo F, Baselga J. Pharmacodynamic studies with the epidermal growth factor receptor tyrosine kinase inhibitor ZD1839. Semin Oncol 2001;28:56–66.
33. Albanell J, Codony-Servat J, Rojo F, et al. Activated extracellular signal-regulated kinases: association with epidermal growth factor receptor/transforming growth factor-α expression in head and neck squamous carcinoma and inhibition by anti-epidermal growth factor receptor treatments. Cancer Res 2001;61:6500–10.
34. Baselga J, Rischin D, Ranson M, et al. Phase I safety, pharmacokinetic, and pharmacodynamic trial of ZD1839, a selective oral epidermal growth factor receptor tyrosine kinase inhibitor, in patients with five selected solid tumor types. J Clin Oncol 2002;20:4292–302.
35. Klapper LN, Waterman H, Sela M, Yarden Y. Tumor-inhibitory antibodies to HER-2/ErbB-2 may act by recruiting c-Cbl and enhancing ubiquitination of HER-2. Cancer Res 2000;60:3384–8.
36. Grandis JR, Drenning SD, Zeng Q, et al. Constitutive activation of Stat3 signaling abrogates apoptosis in squamous cell carcinogenesis *in vivo*. Proc Natl Acad Sci U S A 2000;97:4227–32.
37. Hsieh SS, Malerczyk C, Aigner A, Czubayko F. ERbB-2 expression is rate-limiting for epidermal growth factor-mediated stimulation of ovarian cancer cell proliferation. Int J Cancer 2000;86:644–51.
38. Robert F, Ezekiel MP, Spencer SA, et al. Phase I study of anti-epidermal growth factor receptor antibody cetuximab in combination with radiation therapy in patients with advanced head and neck cancer. J Clin Oncol 2001;19:3234–43.
39. Freireich EJ, Gehan EA, Rall DP, Schmidt LH, Skipper HE. Quantitative comparison of toxicity of anticancer agents in mouse, rat, hamster, dog, monkey, and man. Cancer Chemother Rep 1966;50:219–44.
40. Luo FR, Yang Z, Camuso A, et al. Pharmacokinetics- and pharmacodynamics-guided optimization of the dose and treatment schedule for the dual SRC/ABL inhibitor BMS-354825. ASH 46th Annual Meeting; 2004.
41. Skvortsov S, Sarg B, Loeffler-Ragg J, et al. Different proteome pattern of epidermal growth factor receptor-positive colorectal cancer cell lines that are responsive and nonresponsive to C225 antibody treatment. Mol Cancer Ther 2004;3:1551–8.
42. Khambata-Ford S. Pharmacogenomic approaches for identifying markers predictive of tumor response to Cetuximab (Erbitux). AACR 95th Annual Meeting; 2004.
43. Gao J. Protein profiling approaches to identify predictive markers of tumor response to Cetuximab (Erbitux) using xenograft models. AACR 96th Annual Meeting; 2005.

Clinical Cancer Research

Prediction of Active Drug Plasma Concentrations Achieved in Cancer Patients by Pharmacodynamic Biomarkers Identified from the Geo Human Colon Carcinoma Xenograft Model

Feng R. Luo, Zheng Yang, Huijin Dong, et al.

Clin Cancer Res 2005;11:5558-5565.